

SPONTANEOUS CURRENT-LAYER FRAGMENTATION AND CASCADING RECONNECTION IN SOLAR FLARES: II. RELATION TO OBSERVATIONS

MIROSLAV BÁRTA^{1,2,3}, JÖRG BÜCHNER¹, MARIAN KARLICKÝ², AND PAVEL KOTRČ²

¹Max Planck Institute for Solar System Research, D-37191 Katlenburg-Lindau, Germany

²Astronomical Institute of the Academy of Sciences of the Czech Republic, CZ-25165 Ondřejov, Czech Republic

³Observatory Vlašim, CZ-25801 Vlašim, Czech Republic

Draft version January 18, 2011

ABSTRACT

In the paper by Bárta et al. (ApJ, 2010) the authors addressed some open questions of the CSHKP scenario of solar flares by means of high-resolution MHD simulations. They focused, in particular, on the problem of energy transfer from large to small scales in decaying flare current sheet (CS). Their calculations suggest, that magnetic flux-ropes (plasmoids) are formed in full range of scales by a cascade of tearing and coalescence processes. Consequently, the initially thick current layer becomes highly fragmented. Thus, the tearing and coalescence cascade can cause an effective energy transfer across the scales. In the current paper we investigate whether this mechanism actually applies in solar flares. We extend the MHD simulation by deriving model-specific features that can be looked for in observations. The results of the underlying MHD model showed that the plasmoid cascade creates a specific hierarchical distribution of non-ideal/acceleration regions embedded in the CS. We therefore focus on the features associated with the fluxes of energetic particles, in particular on the structure and dynamics of emission regions in flare ribbons. We assume that the structure and dynamics of diffusion regions embedded in the CS imprint themselves into structure and dynamics of flare-ribbon kernels by means of magnetic-field mapping. Using the results of the underlying MHD simulation we derive the expected structure of ribbon emission and we extract selected statistical properties of the modelled bright kernels. Comparing the predicted emission and its properties with the observed ones we obtain a good agreement of the two.

Subject headings: Sun: flares — Sun: magnetic reconnection — Sun: electron acceleration

1. INTRODUCTION

For many years the common picture of solar eruptions and flares is based on the CSHKP model (see Magara et al. 1996, and references therein). It involves reconnection in a global vertical flare current layer formed behind ejected flux-rope/filament (Lin & Forbes 2000, and references therein). The standard model is in good agreement with observed large-scale dynamics of eruptive events. Several question, however, remain open. In particular, it is not clear, by which mechanism the energy accumulated in relatively large-scale (≈ 1000 km) structures of magnetic field associated with the flare CS is transferred towards the small dissipation scales. Indeed, the magnetic diffusion in the almost collisionless solar coronal plasma is an essentially kinetic process at scales of the order $d_i = c/\omega_{pi}$ (Büchner 2006). Another open question is the relation between the well-organised dynamics of solar eruptions observed at large scales and the HXR and radio signatures of fragmented energy release (Aschwanden 2002; Karlický et al. 2000). And finally, the CSHKP model has been put in question by many authors (e.g. Vlahos 2007), in particular because its apparent incapability to explain the large fluxes of accelerated particles inferred from HXR observations.

Recently – in order to address the issue of energy transfer across the broad range of MHD scales – Bárta et al. (2010) [in further text referred as *Paper I*] investigated magnetic reconnection in an extended current layer by means of high-resolution MHD simula-

tion. Inspired by the “*fractal reconnection*” conjecture of Shibata & Tanuma (2001) the authors of Paper I performed a 2.5D numerical simulation covering large range of MHD scales. They conjectured, that – in analogy with the vortex-tube cascade in fluid dynamics – a cascade of magnetic flux-tubes from large to small scale can provide the mechanism for energy transfer across the scales. Two mechanisms of fragmentation were identified in Paper I: (1) The tearing cascade – in line with concept of *fractal reconnection* by Shibata & Tanuma (2001), developed recently into the theory of *chain plasmoid instability* by Loureiro et al. (2007) and Uzdensky et al. (2010), supported further by numerical MHD simulations by Bhattacharjee et al. (2009), Samtaney et al. (2009), and Huang & Bhattacharjee (2010) and, (2) ambient-field driven coalescence of flux-ropes/plasmoids leading to formation of transversal current sheets subjected further to the same chain of processes of cascading fragmentation. Extrapolation of the results leads to the picture in which the plasmoid cascade continues down to the kinetic scale where actual magnetic dissipation and particle acceleration occurs, most likely via the kinetic coalescence of plasmoids (Drake et al. 2005; Karlický et al. 2010). Nevertheless, other processes can appear in the range between MHD and plasma kinetic scales, e.g., the Hall type of reconnection – see recent simulations by Shepherd & Cassak (2010) and Huang et al. (2010).

As it has been shown in the Paper I, cascading reconnection forms multiple non-ideal regions (at the resolution limit – see discussion in Paper I) hierarchically distributed in the fragmenting current layer. As a re-

sult, the open questions of energy transfer, fragmented vs. organised flare energy release, and particle acceleration seem to be closely related to each other in the presence of cascading reconnection.

The question arises, whether this mechanism found by simulations is relevant for actual solar flares. We address this topic in our present paper. For this sake we derive critical signatures specific to the model developed in Paper I, that allow comparison with observations. It is currently impossible to observe small-scale magnetic structures, whose formation in the fragmented flare current layer is predicted by the cascading-reconnection model, directly. Almost all information on the impulsive phase of flares comes from the radiation emitted by accelerated particles. Therefore we concentrate on such predictions of the MHD model that are connected with specific distribution and dynamics of acceleration regions in the fragmenting flare current layer.

In particular, by magnetic mapping of non-ideal regions embedded in the current sheet to the photosphere we derive expected consequences of the distribution and dynamics of acceleration regions for flare ribbons. Using the results of underlying MHD model presented in Paper I we qualitatively derive the structure and dynamics of expected ribbon emission. We compare the modelled ribbon structure with observations directly and by means of its statistical properties used by Nishizuka et al. (2009).

The paper is organised as follows: First, in Section 2.1, we briefly summarise the results of the underlying high-resolution MHD simulation of cascading reconnection. Then, in Section 2.2 we present the extension of underlying MHD model utilised to produce model-specific results/consequences in the form able to be directly compared with observations. In particular, we study the distribution and dynamics of dissipative/acceleration regions, represented by the embedded X-points, and their magnetic mapping to the chromosphere/photosphere of the Sun. For obtained dynamics of acceleration regions and their magnetic foot-points we qualitatively model the expected emission of flare ribbons (Section 3). We compare the emission structure of modelled and observed ribbons. Furthermore, we extract selected statistical properties of emission kernels embedded in modelled ribbons and compare them with the results found by analysis of actual ribbon observations (Nishizuka et al. 2009). Finally, in Section 4 we discuss our results with the intention to evaluate the relevance of cascading reconnection/fragmentation processes presented in Paper I for actual solar flares.

2. MODEL

In this section we describe the procedures allowing to simulate observable signatures specific to cascading reconnection. For clarity we first briefly summarise the main features of current-layer fragmentation model (Paper I).

2.1. Basic MHD model

In Paper I the authors studied cascading reconnection and energy transfer from accumulation (large) to dissipation (small) scales. They used a high-resolution MHD model with a non-ideal, resistive term depending on the current-carrier drift velocity

v_D as

$$\eta(\mathbf{r}, t) = \begin{cases} 0 & : |v_D| \leq v_{cr} \\ C \frac{(v_D(\mathbf{r}, t) - v_{cr})}{v_0} & : |v_D| > v_{cr} \end{cases} \quad (1)$$

with the threshold v_{cr} set to the higher, more realistic value corresponding to increased resolution. The authors applied the model to the large-scale vertical current sheet in solar eruptive flares.

The simulations in Paper I have been performed in dimensionless variables: Spatial coordinates x , y , and z has been expressed in units of the current sheet half-width L_A at the photospheric level ($z = 0$) and the time has been normalised to the Alfvén transit time $\tau_A = L_A/V_{A,0}$, where $V_{A,0} = B_0/\sqrt{\mu_0\rho_0}$ is the asymptotic value ($x \rightarrow \infty, z = 0$) of the Alfvén speed at $t = 0$. In order to relate the model to real solar conditions appropriate scaling has been adopted in Paper I. Based on the gravity-introduced scale-height relation $L_A = 600$ km has been found. Due to this relation both the dimensionless and SI units can be used further in our present paper.

In Paper I the authors described how tearing and driven coalescence instabilities lead to the fragmentation of an originally unstructured flare current layer. As a consequence a cascade of magnetic flux-ropes/plasmoids is formed from large to consecutively smaller scales. The structuring of the current layer leads to formation of multiple thin embedded current sheets. They can host non-ideal regions where particles can be accelerated. Enhanced numerical resolution revealed the structure of dissipation regions: They form many thin channels of non-zero magnetic diffusivity. The spatial distribution and dynamics of these diffusivity channels has been further studied via tracking of the X-points associated with the non-ideal regions. Analysis shows hierarchically-structured grouping of the dissipation channels and intermittency in their life-times and times for which they are magnetically connected to the photosphere.

The structure, distribution and dynamics of the non-ideal regions should be reflected in specific observable features that we are going to derive in the following subsection.

2.2. Derivation of model-specific observable features

Unfortunately, it is impossible to directly measure the magnetic field or current density in the coronal current sheets (and at all not with the resolution reached in the simulation done in Paper I). Hence, we need some indirect, more subtle comparison between observed and modelled quantities. A possible way which may lead to indirect indication of current-sheet fragmentation has recently been presented by Nishizuka et al. (2009). These authors study the structure of emission in flare ribbons, namely the distribution and dynamics of embedded bright kernels. They conjecture possible relation of the resulting power-law distributions found in their statistical analysis of ribbon-kernel properties with the concept of *fractal current sheet* (Shibata & Tanuma 2001).

We follow this idea from the other end. We start with the structure, distribution, and dynamics of diffusion/acceleration regions that are specific to the cascading-reconnection model as they have been found in Paper I. Then, we relate these features to the structure and dynamics of emission in flare ribbons. We proceed as

follows: As shown in Paper I (Fig. 6), the reconnection X-points are associated with thin channels of magnetic diffusivity. Hence, we take the X-points as geometric representatives of dissipation regions. In these regions electrons can be accelerated, e.g., by the DC electric fields. However, also different acceleration mechanisms has been proposed – e.g. Drake et al. (2005) suggest Fermi-type acceleration in contracting plasmoids. We can include this type of acceleration into account by following consideration: Extrapolating the results of numerical simulations of reconnection cascade to smaller scales one can imagine, that each dissipative region surrounding studied X-point in fact contains many unresolved small-scale magnetic islands. Electron acceleration in these non-ideal regions is then performed (in line with ideas by Drake et al. 2005) via coalescence and shrinkage of these micro-plasmoids. Anyway, electrons accelerated by Fermi-type mechanism inside the plasmoids are trapped and can be released to the open field (which connects CS to chromosphere) again in the vicinity of the X-points, where they become demagnetized. For further drelated discussion on electron acceleration in magnetic islands see, e.g. Oka et al. (2010).

In our study we focus on electrons as we are interested in optical and UV/EUV chromospheric response ascribed to electron beams. These are then transported along the magnetic field lines either up-ward to the solar corona or downward, until they reach dense layers of the solar atmosphere, where their energy is thermalized. Here we concentrate on the down-ward transported electrons. In order to study the positions and dynamics of the points, where these electrons reach the chromosphere, i.e. the expected bright kernels, we map found X-points to the bottom boundary of the simulation box using magnetic field. The magnetic field lines that go through given X-point represent magnetic separatrices in our 2D model. Therefore, we are seeking for intersections of magnetic separatrices with the bottom boundary. In the following we will refer to this footpoints at the bottom boundary as to *kernels*. Thus, from known position of all X-points (Fig. 7 in Paper I) and knowing the magnetic field we can calculate the positions $x_k(t)$ of all kernels k for each recorded time step t of the simulation. Note, that due to the 2D geometry of the model the foot-point/kernel position is uniquely given by its x -coordinate (see Paper I for details).

The calculations of the chromospheric emission in a certain spectral line (e.g. H_α or C IV) in response to the bombardment of electrons accelerated in a distant reconnection region is a difficult task (Kašparová et al. 2009; Varady et al. 2010). In order to obtain an at least qualitative output that could be later compared with observations we use for ribbon-intensity distribution the expression

$$I_k(x, y, t) = I_0 \exp \left(-\frac{(x - x_k(t))^2}{\Delta^2} \right) \\ I(x, y, t) = \sum_k I_k(x, y, t), \quad (2)$$

instead of description of all the complicated processes of electron transport, energy deposition, chromospheric response, and radiative transfer. The intensity I is summed over all kernels k ; y is the second (however invariant in

our model) coordinate in the photosphere. The kernel size is set to $\Delta = 0.1L_A$. Since the model is capable neither to estimate the electron-beam flux nor the energy thermalized in the kernel we set the intensity scale to $I_0 = 1$. We will return to this point later in the discussion.

Let us now apply this procedures to the results of simulations presented in Paper I.

3. RELATION TO OBSERVATIONS

Fig. 1 depicts the above-described procedure of mapping of X-points to the photosphere along magnetic separatrices and flare-ribbon emission calculation. Obtained results are shown for $t = 391.5\tau_A$. Panels (a) – (c) show how three dissipative regions/X-points embedded in the fragmented current layer are magnetically connected to the bottom boundary and mapped by separatrices to the positions $x \approx \pm 2800$ km (one kernel) and $x \approx \pm 3750$ km (two mutually close kernels).

A view at the flare ribbons obtained by applying the simple model described by Eq. (2) is presented in Fig. 1(d). As the figure indicates, in some cases one can observe even multiple pairs of flare ribbons. This is close to the idea of chromospheric re-brightening studied by Miklenic et al. (2010). The inner separatrix associated with the internal pair of ribbons is connected to the X-point which appeared temporarily in the transversal current sheet formed between merging plasmoid and the loop arcade (see also Fig. 4 in Paper I). Figs. 1(e) and (f) show the emission intensity profile along the x -axis calculated according to the model in Eq. (2). The enlarged detail shown in Fig. 1(f) reveals an internal double-peak structure of the outer ribbons. Note, that a similar structuring is seen in observed H_α ribbons (Fig. 2).

In order to study the dynamics of kernels and associated X-points during the entire recorded interval of evolution ($300\tau_A - 400\tau_A$) we tracked the moving positions of all X-points and the magnetically-associated (mapped) kernels. Kinematics of the kernels (foot-points of separatrices) is depicted in Fig 3. Panel 3(a) presents a global picture of kernel dynamics over the entire recorded interval. Because of the CS symmetry only the right ribbon positions are displayed. The spatial coordinate x , the distance from the polarity-inversion line (PIL), is limited to the interval where the kernels actually occur. Fig 3(b) shows a detailed view of the area selected in panel (a). In order to reach higher zoom the global trend (motion) of the group of kernels (i.e. the increasing ribbon separation as the flare proceeds) has been subtracted by applying the transformation $\bar{x}/L_A = x/L_A - 0.0125(t/\tau_A - 300)$. X-points that are separated only by tiny magnetic islands can map practically to the same kernel. They then cannot be distinguished even in the zoomed display. Therefore, for each time we take a set of kernel positions (its size varies with time) and display every kernel in different colour. Fig. 3 shows various life-times of the kernels and other aspects of their dynamics, like bifurcation/merging. Note, that the life-time of the kernel is not determined solely by the life-time of the associated distant X-point but also by the processes in the current layer that can change the magnetic connectivity of diffusion regions embedded in the current layer to the photosphere (Fig. 7 in Paper I).

We have further extracted selected characteristics of

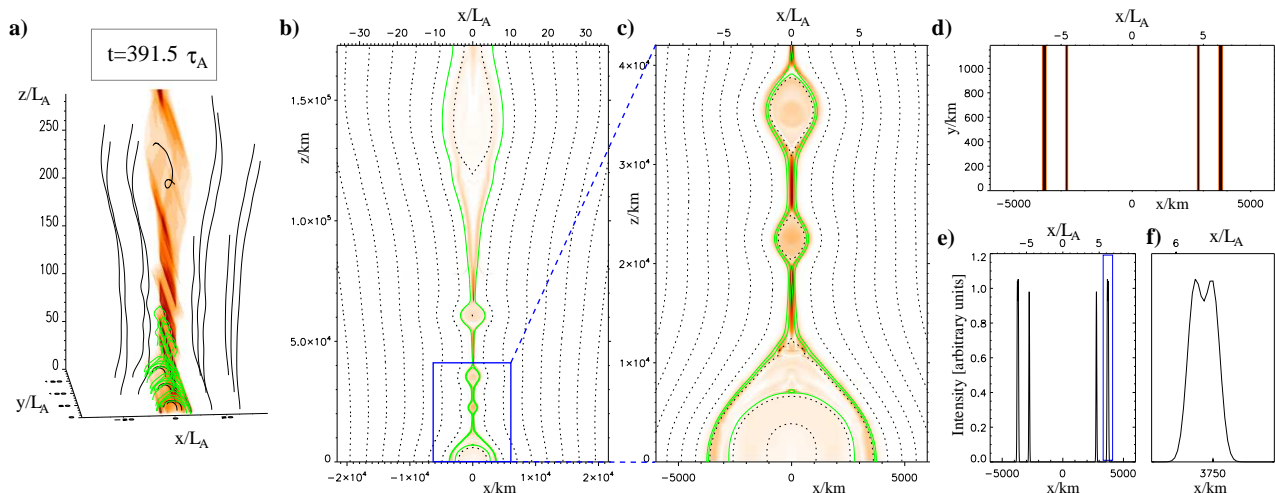


FIG. 1.— Model-specific consequences of cascading magnetic reconnection. (a) Global 3D magnetic and current-density structures at $t = 391.5\tau_A$. The magnetic field (black lines), the separatrixes that map the diffusive regions to the bottom boundary (green lines), and the current density (red colour scale) are shown. (b) Projection of (a) into the xz -plane. The x -axis shows positions both in the units of L_A (top) and in kilometres according to the scaling adopted in Section 2.1. (c) Enlarged view of the selected rectangle reveals double-structure of the outer pair of separatrixes hitting the bottom boundary near $x \pm 3750$ km. (d) Modelled view at two pairs of flare emission ribbons (inverted colour scale, darker means higher intensity here). (e) Modelled emission profiles across the ribbons. (f) Detailed view of the outer-ribbon profile reveals its internal double-peaked structure.

the modelled kernel dynamics and compare them with the observations of Nishizuka et al. (2009). For this sake we processed our model results in the same manner as those authors by binning photosphere along the x -axis. For the bin size we chose $\Delta x = 0.05L_A$. For each time we integrated the intensity given by Eq. (2) over each bin. Thus we obtained a proxy for “light-curves” of all bins. Fig. 4 shows three examples of such light-curves for bins centred around positions $x = 4.58L_A$ (2750 km), $x = 4.93L_A$ (2950 km), and $x = 5.73L_A$ (3435 km). Narrow peaks coming from the short-living X-points are superimposed over the longer living bright kernels (c.f. Fig. 2(b) in Nishizuka et al. 2009).

As in Nishizuka et al. (2009), we then determined the peaks at each light-curve and recorded their time of occurrence and their maximum intensity. We calculated the statistical distributions of the peak intensities and the time-intervals between two subsequent peaks. The results of this analysis are presented in Fig. 5. Despite of the poor statistics (for our 1D mesh we identified only 68 peaks) we obtained spectral indices $s = -1.48$ for the peak-intensity (panel 5(a)) and $s = -1.73$ for the time interval between subsequent peaks (Fig. 5(b)).

4. DISCUSSION AND CONCLUSIONS

The ‘standard’ CSHKP picture of solar eruptive flares involves the formation of a global flare current sheet (CS) behind a ejected filament followed by magnetic reconnection in this CS. Nevertheless, deeper study of this scenario invokes further questions: 1) How is the energy accumulated in flares in relatively large-scale structures (global flare current layer) transferred to the dissipative (kinetic) scales, 2) How can we observe regular dynamics in eruption/flare on large scales, just in line with the CSHKP scenario, and the signatures of fragmented energy release at the same moment, and 3) How can the large fluxes of accelerated electrons inferred from HXR observations be reconciled with a single, relatively small diffusion region assumed in classical CSHKP model.

The simulations presented in Paper I showed, that a cascading reconnection resulting from the formation and interaction of plasmoids/flux-ropes can address these three fundamental questions at once and that it might provide viable scenario for magnetic energy dissipation in large-scale systems, like solar (eruptive) flares.

In the present paper we evaluated the relevance of this model for actual solar flares. For this sake we derived observable model predictions that are specific for the cascading-reconnection scenario, and searched for the predicted features in observed data. Since multiple acceleration regions embedded in the global flare current layer are – via magnetic field-line mapping – inherently connected with the structured emission in the flare ribbons, detailed study of the ribbon kernels might bring some evidence for the cascading processes in the current layer above the flaring region. This idea is illustrated by Fig. 1 which shows the structuring of modelled emission in ribbons. Fig. 1 further indicates, that the larger-scale plasmoid interacting with the flare-loop arcade can temporarily form a second pair of ribbons. The plasmoid/loop-arcade interaction may play significant role in flare dynamics. Another indirect evidence of such interaction based on analysis of series of X-ray images of the limb flare has been presented by Kolomański & Karlický (2007) and Milligan et al. (2010).

Similar structuring of H_α emission as presented in Figs. 1(d)–(f) is, indeed, visible in Fig. 2. Yet another interesting feature in Fig. 2 is the dark filament-like structure (indicated by an arrow). Since the original large-scale filament whose eruption initiated the flare was already far away at the time of observation, the absorption feature can be interpreted as a manifestation of one of the secondary plasmoids formed in the global current layer in line with the presented cascading-fragmentation scenario. The secondary plasmoids represent enhanced-density structures. Density increase in connection with

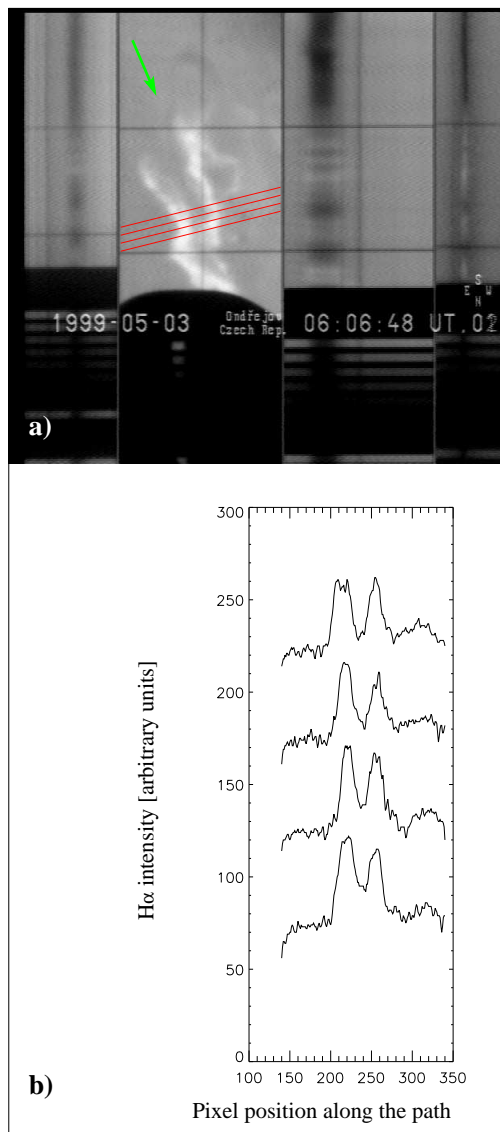


FIG. 2.— Observation of flare H_α emission ribbons (a) and profiles of H_α intensity (b) along selected paths (red lines in the panel (a)). The ribbon emission is structured (double-peaked?) – c.f. Fig. 1. The green arrow points to the filament-like dark structure which projects to the space between flare ribbons.

consequent faster radiative cooling might lead to the detectable H_α absorption. The secondary plasmoid can be consequently manifested as a darker feature at the background of relatively brighter chromosphere.

A sophisticated study of the structure of flare ribbons was presented by Nishizuka et al. (2009). These authors studied the statistical properties of emission kernels found inside the ribbons and they found a power-law distribution of the studied kernel characteristics. A power-law distribution can be a signature of self-organised criticality evolution (Aschwanden 2002; Vlahos 2007). It can also indicate a *fractal current sheet* decay (Shibata & Tanuma 2001). The latter scenario is in fact favoured by the subsequent analysis of Nishizuka et al. (2010) which relates the energy release measured by means of HXR flux and ejection of multiple plasmoids formed in the fragmenting current sheet.

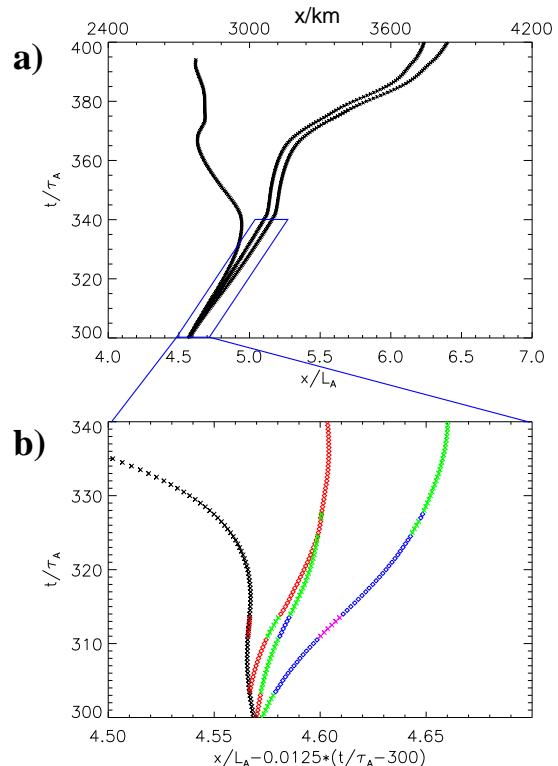


FIG. 3.— Kinematics of flare ribbon kernels obtained by magnetic mapping of dissipation regions in cascading reconnection down to the photosphere. (a) View of all kernel positions in $t=300 \tau_A$ — $400 \tau_A$. Abscissa positions in kilometres (upper scale) and in units of L_A . (b) Detailed view of the area selected in (a) (the blue rhomboid). The global motion of the group of kernels has been subtracted in order to reach larger zoom. For each time instant each kernel is depicted by unique color in order to distinguish between close (almost overlapping) kernels/foot-points.

In our present paper we have established the connection between the hierarchical distribution of diffusion regions formed by cascading reconnection and the statistical properties of emission kernels from first principles. We have studied the dynamics (positions, and the mechanisms and times of creation/annihilation) of O- and X-type points in the current layer as well as of the kernel-points associated with the diffusion regions (X-points) by means of magnetic field-line mapping. We then associated each found kernel with the emission according to Eq. (2). We chose this simple model as we do not have any information about the accelerated electron fluxes absorbed in the kernel, nor can we easily calculate the chromospheric response in terms of (e.g., H_α) emission. Our choice of the unified peak intensity $I_0 = 1$ for all kernels can be justified following way: After all, the particle acceleration is performed by kinetic processes at the small-scale end of the cascade. Suggested mechanism (see e.g. Drake et al. 2005) involves, e.g. kinetic coalescence and shrinkage of small-scale magnetic islands/plasmoids. In the dissipative range of scales the slope of the energy spectrum (see Fig. 1 in Paper I) is very steep. Hence, the size of plasmoids at kinetic scale can be expected more or less uniform as indicated also by PIC simulations. In such case the elementary injections of accelerated particles are, perhaps, roughly of the same magnitude. The intermittent, spiky structure of observed emission pro-

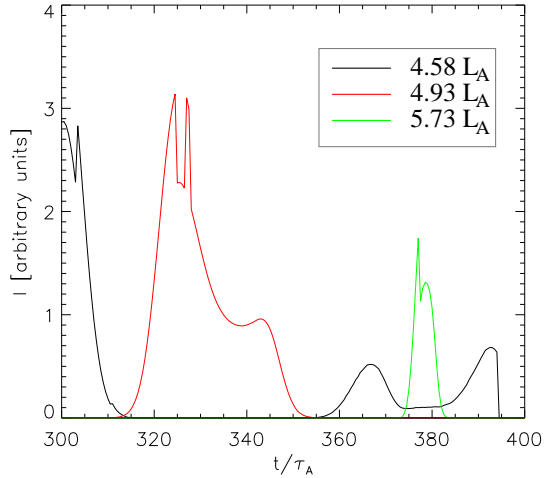


FIG. 4.— Modelled light-curves for three selected bins at positions $x = 4.58L_A$ (2750 km), $x = 4.93L_A$ (2950 km), and $x = 5.73L_A$ (3435 km).

files is then the result of overlapping of many of these elementary injection peaks (Aschwanden 2002). Indeed, we observe this feature in examples of the modelled light-curves obtained at fixed points at the bottom boundary (Fig. 4). Despite of the intensity produced by the elementary particle injection being normalised to $I_0 = 1$, the overlapping elementary peaks produce spiky intensity profiles ranging from $I = 0$ to $I > 3$.

In order to directly compare our results with the findings of Nishizuka et al. (2009) we have performed the same statistical analysis of the peaks in our artificial light-curves. We have found the statistical distributions of the emission peak intensities and of the time-lag between subsequent emission peaks (Fig. 5). Because of the 2-D geometry of underlying MHD model we have obtained 1-D distribution of emission kernels. Consequently we have found smaller number of the peaks. Despite of the resulting poor statistics we could conclude, that the slopes of the power-law distributions obtained by our model agree surprisingly well with those found by Nishizuka et al. (2009) for observed light-curves: For the statistical distribution of the peak intensities we have found spectral index $s = -1.48$ (Nishizuka et al. (2009) obtained $s = -1.5$) and for the time-lag between peaks we obtained $s = -1.74$ ($s = -1.8$ in Nishizuka et al. (2009)). We are aware that our statistics is, however, rather poor as it operates with only 68 peaks found in total. Thus, it would be premature to take this agreement as conclusive. Nevertheless the result indicates that the statistical properties of emission kernels resulting from cascading reconnection and of those observed are – at least – not in direct contradiction.

Results of presented comparison between the modelled features attributed specifically to cascading reconnection and their observed counterparts supports – in our view – the relevance of cascading reconnection processes studied in Paper I for reconnection in solar atmosphere. Agreements found between the statistical properties of modelled and observed emission kernels invokes, however, further questions. The underlying 2.5D MHD model ig-

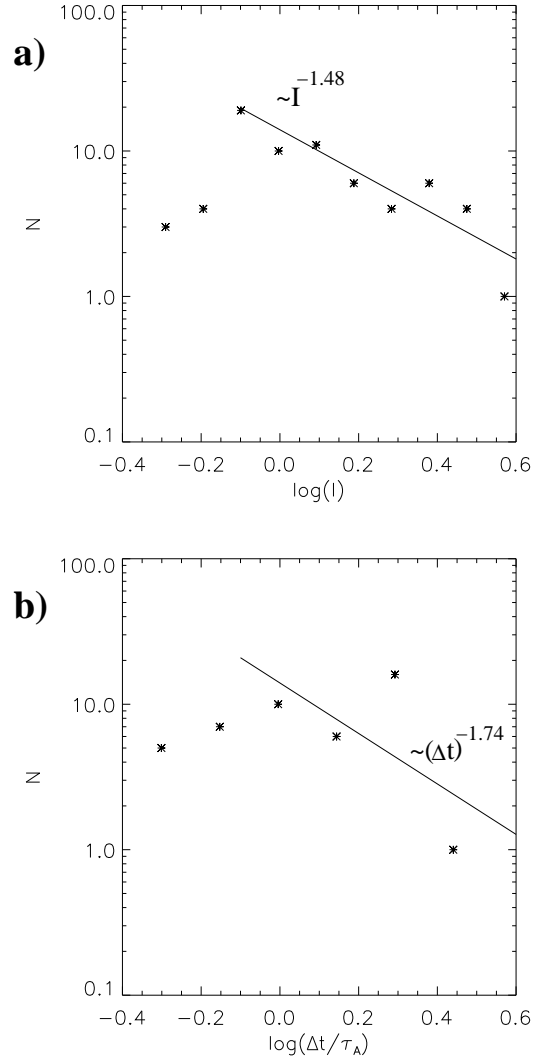


FIG. 5.— Statistical distribution of the modelled intensity (a) and the time-interval between subsequent emission peaks (b) for accumulated light-curves from all mesh-boxes. N indicates the number of peaks with the property within the bin.

nores structuring of the current sheet in the y -direction (along the PIL). This result might indicate that modes with $k_y > 0$ (in the off-plane direction) may not play too significant role in current-layer fragmentation in solar flares, or at least, that they do not reach the smallest scales to substantially influence the dynamics (life-time) of kinetic-scale diffusion regions. This issue can be addressed, however, only within the framework of a full 3D MHD model.

This research was performed under the support of the European Commission through the SOLAIRE Network (MTRN-CT-2006-035484) and the grants P209/10/1680, 205/09/1469, 205/09/1705, P209/10/1706 of the Grant Agency of the Czech Republic, by the grant 300030701 of the Grant Agency of the Czech Academy of Science, and the research project AV0Z10030501 of Astronomical Institute of the Czech Academy of Science.

The authors thanks to anonymous referee, whose com-

ments where very helpful in improving quality of the paper.

REFERENCES

- Aschwanden, M. J. 2002, *Space Sci. Rev.*, 101, 1
- Bárta, M., Büchner, J., Karlický, M., & Skála, J. 2010, *ApJ*, submitted, 1011.4035
- Bhattacharjee, A., Huang, Y., Yang, H., & Rogers, B. 2009, *Physics of Plasmas*, 16, 112102, 0906.5599
- Büchner, J. 2006, *Space Science Reviews*, 124, 345
- Drake, J. F., Shay, M. A., Thongthai, W., & Swisdak, M. 2005, *Physical Review Letters*, 94, 095001.1
- Huang, Y., & Bhattacharjee, A. 2010, *Physics of Plasmas*, 17, 062104, 1003.5951
- Huang, Y.-M., Bhattacharjee, A., & Sullivan, B. P. 2010, *ArXiv e-prints*, 1010.5284
- Karlický, M., Bárta, M., & Rybák, J. 2010, *A&A*, 514, A28+
- Karlický, M., Jiříčka, K., & Sobotka, M. 2000, *Sol. Phys.*, 195, 165
- Kašparová, J., Varady, M., Heinzl, P., Karlický, M., & Moravec, Z. 2009, *A&A*, 499, 923, 0904.2084
- Kołomański, S., & Karlický, M. 2007, *A&A*, 475, 685
- Lin, J., & Forbes, T. G. 2000, *J. Geophys. Res.*, 105, 2375
- Loureiro, N. F., Schekochihin, A. A., & Cowley, S. C. 2007, *Physics of Plasmas*, 14, 100703, arXiv:astro-ph/0703631
- Magara, T., Mineshige, S., Yokoyama, T., & Shibata, K. 1996, *ApJ*, 466, 1054
- Miklenic, C. H., Veronig, A. M., Vršnak, B., & Bárta, M. 2010, *ApJ*, 719, 1750
- Milligan, R. O., McAteer, R. T. J., Dennis, B. R., & Young, C. A. 2010, *ApJ*, 713, 1292, 1003.0665
- Nishizuka, N., Asai, A., Takasaki, H., Kurokawa, H., & Shibata, K. 2009, *ApJ*, 694, L74
- Nishizuka, N., Takasaki, H., Asai, A., & Shibata, K. 2010, *ApJ*, 711, 1062
- Oka, M., Phan, T., Krucker, S., Fujimoto, M., & Shinohara, I. 2010, *ApJ*, 714, 915, 1004.1154
- Samtaney, R., Loureiro, N. F., Uzdensky, D. A., Schekochihin, A. A., & Cowley, S. C. 2009, *Physical Review Letters*, 103, 105004, 0903.0542
- Shepherd, L. S., & Cassak, P. A. 2010, *Physical Review Letters*, 105, 015004, 1006.1883
- Shibata, K., & Tanuma, S. 2001, *Earth, Planets, and Space*, 53, 473, arXiv:astro-ph/0101008
- Uzdensky, D. A., Loureiro, N. F., & Schekochihin, A. A. 2010, *Physical Review Letters*, 105, 235002, 1008.3330
- Varady, M., Kašparová, J., Moravec, Z., Heinzl, P., & Karlický, M. 2010, *IEEE Transactions on Plasma Science*, 38, 2249
- Vlahos, L. 2007, in *Lecture Notes in Physics*, Berlin Springer Verlag, Vol. 725, *Lecture Notes in Physics*, Berlin Springer Verlag, ed. K.-L. Klein & A. L. MacKinnon, 15–31